

Integrating Metaheuristics *in* Computer Vision *for* Real-World Optimization Problems

Edited by

Kapil Joshi, Shubham Mahajan,
Amit Kant Pandit, and Nitish Pathak

 Scrivener
Publishing

WILEY

Integrating Metaheuristics in Computer Vision for Real- World Optimization Problems

Scrivener Publishing

100 Cummings Center, Suite 541J
Beverly, MA 01915-6106

Publishers at Scrivener

Martin Scrivener (martin@scrivenerpublishing.com)
Phillip Carmical (pcarmical@scrivenerpublishing.com)

Integrating Metaheuristics in Computer Vision for Real- World Optimization Problems

Edited by

Shubham Mahajan

School of Engineering, Ajeenkya D Y Patil University, Pune, Maharashtra, India

Kapil Joshi

*Department of Computer Science & Engineering, Uttarakhand Institute of Technology,
Dehradun, India*

Amit Kant Pandit

Shri Mata Vaishno Devi University, Katra, India

and

Nitish Pathak

*Department of Information Technology, Bhagwan Parshuram Institute of Technology,
New Delhi, India*



WILEY

This edition first published 2024 by John Wiley & Sons, Inc., 111 River Street, Hoboken, NJ 07030, USA and Scrivener Publishing LLC, 100 Cummings Center, Suite 541J, Beverly, MA 01915, USA

© 2024 Scrivener Publishing LLC

For more information about Scrivener publications please visit www.scrivenerpublishing.com.

All rights reserved. No part of this publication may be reproduced, stored in a retrieval system, or transmitted, in any form or by any means, electronic, mechanical, photocopying, recording, or otherwise, except as permitted by law. Advice on how to obtain permission to reuse material from this title is available at <http://www.wiley.com/go/permissions>.

Wiley Global Headquarters

111 River Street, Hoboken, NJ 07030, USA

For details of our global editorial offices, customer services, and more information about Wiley products visit us at www.wiley.com.

Limit of Liability/Disclaimer of Warranty

While the publisher and authors have used their best efforts in preparing this work, they make no representations or warranties with respect to the accuracy or completeness of the contents of this work and specifically disclaim all warranties, including without limitation any implied warranties of merchant-ability or fitness for a particular purpose. No warranty may be created or extended by sales representatives, written sales materials, or promotional statements for this work. The fact that an organization, website, or product is referred to in this work as a citation and/or potential source of further information does not mean that the publisher and authors endorse the information or services the organization, website, or product may provide or recommendations it may make. This work is sold with the understanding that the publisher is not engaged in rendering professional services. The advice and strategies contained herein may not be suitable for your situation. You should consult with a specialist where appropriate. Neither the publisher nor authors shall be liable for any loss of profit or any other commercial damages, including but not limited to special, incidental, consequential, or other damages. Further, readers should be aware that websites listed in this work may have changed or disappeared between when this work was written and when it is read.

Library of Congress Cataloging-in-Publication Data

ISBN 978-1-394-23092-1

Cover image: Pixabay.Com

Cover design by Russell Richardson

Set in size of 11pt and Minion Pro by Manila Typesetting Company, Makati, Philippines

Printed in the USA

10 9 8 7 6 5 4 3 2 1

Contents

| | |
|---|-----------|
| Preface | xv |
| 1 Advancement in Diagnostic and Therapeutic Techniques for Ischemic Stroke | 1 |
| <i>Mukul Jain, Divya Patil, Shubham Gupta and Shubham Mahajan</i> | |
| 1.1 Introduction | 2 |
| 1.2 Diagnostic Tools of Ischemic Stroke | 4 |
| 1.2.1 Preimaging | 4 |
| 1.2.2 Imaging | 4 |
| 1.2.2.1 Computed Tomography Scan | 4 |
| 1.2.2.2 Magnetic Resonance Imaging | 5 |
| 1.2.2.3 Electromyography | 6 |
| 1.2.2.4 Electroencephalography (EEG) | 6 |
| 1.2.2.5 Positron Emission Tomography (PET) | 6 |
| 1.3 Artificial Intelligence–Based Diagnostic Tools | 7 |
| 1.4 Blood-Based Protein Biomarker for Stroke | 8 |
| 1.5 Markers for Endothelial Damage | 8 |
| 1.6 Markers of Brain Injury | 9 |
| 1.7 Therapeutic Advances in Ischemic Stroke | 9 |
| 1.7.1 Ligand-Mediated Active Targeting | 9 |
| 1.7.2 Nanomedicines That Provide Oxygen to Ischemic Brain Tissue | 10 |
| 1.7.3 Reducing Oxidative Stress With Nanomedicines | 10 |
| 1.7.4 Multiple Abnormalities are Controlled by Nanomedicine | 10 |
| 1.8 Nanoparticles | 11 |
| 1.8.1 Carbon Nanotubes | 11 |
| 1.8.2 Dendrimers | 12 |
| 1.8.3 Metal Nanoparticles | 12 |
| 1.9 Conclusion | 13 |
| Future Perspectives | 13 |
| References | 14 |
| 2 Object Detection and Tracking Face Detection and Recognition | 25 |
| <i>Varsha K. Patil, Pawan Nawade, Rudra Nagarkar and Paresh Kadale</i> | |
| 2.1 Introduction | 25 |
| 2.2 Motivation | 30 |
| 2.3 The Basics of Computer Vision | 31 |
| 2.3.1 Computer Vision | 31 |

| | | |
|----------|--|-----------|
| 2.3.2 | Implementation of Computer Vision | 31 |
| 2.3.3 | Applications of Computer Vision | 32 |
| 2.3.3.1 | Image Processing Technique | 32 |
| 2.3.3.2 | Feature Extraction and Feature Selection Technique | 33 |
| 2.3.3.3 | Object Recognition Algorithm | 33 |
| 2.4 | Face Detection | 34 |
| 2.4.1 | What is Face Detection | 34 |
| 2.4.2 | Techniques for Face Detection | 34 |
| 2.5 | Facial Expression | 38 |
| 2.5.1 | Facial Recognition | 38 |
| 2.5.2 | Information About Face | 39 |
| 2.5.3 | Algorithms | 40 |
| 2.6 | Object Detection | 41 |
| 2.6.1 | Object Tracking | 41 |
| 2.6.2 | Algorithms Used in Object Detection | 43 |
| 2.7 | Face Detection and Identification in Practical Situations | 44 |
| 2.7.1 | Face Detection | 44 |
| 2.7.2 | Face Detection and Identification in Real-World Situations | 45 |
| 2.8 | Future Direction in Object Detection and Tracking | 47 |
| 2.8.1 | Future Plans for Object Tracking and Detection | 47 |
| 2.8.1.1 | Multiobject Tracking | 48 |
| 2.8.2 | 3D Object Tracking and Detection | 49 |
| 2.8.3 | Real-Time Performance | 50 |
| 2.9 | Conclusion | 52 |
| | References | 53 |
| 3 | Printing Organs with 3D Technology | 55 |
| | <i>Shaik Aminabee</i> | |
| 3.1 | Introduction | 55 |
| 3.2 | Bioprinting in Three Dimensions (3D) | 56 |
| 3.3 | 3D Printing Types | 57 |
| 3.3.1 | Inkjet Bioprinting | 58 |
| 3.3.2 | Microextrusion Bioprinting | 58 |
| 3.3.3 | Laser-Assisted Printing | 59 |
| 3.3.4 | Stereolithography | 59 |
| 3.3.5 | 3D Bioprinting Materials and Cells | 59 |
| 3.4 | Applications for 3D Printing in Cells | 60 |
| 3.4.1 | Blood Vessels | 60 |
| 3.4.2 | Liver | 61 |
| 3.4.3 | Cartilage | 62 |
| 3.4.4 | Muscle | 62 |
| 3.4.5 | Bone | 63 |
| 3.4.6 | Skin | 63 |
| 3.4.7 | Neutralization of Neurons | 64 |
| 3.4.8 | Pancreas | 64 |
| 3.5 | New Developments | 65 |

| | | |
|----------|---|-----------|
| 3.6 | Progress in India | 66 |
| 3.7 | Limitation | 67 |
| 3.8 | A Future Point of View | 67 |
| 3.9 | Conclusion | 68 |
| | References | 68 |
| 4 | Comparative Evaluation of Machine Learning Algorithms for Bank Fraud Detection | 71 |
| | <i>Kiran Jot Singh, Divneet Singh Kapoor, Kunal Ranjan Singh, Chirag Kalucha, Gatik Alagh, Khushal Thakur and Anshul Sharma</i> | |
| 4.1 | Introduction | 71 |
| 4.2 | Proposed Framework | 73 |
| 4.3 | Results | 74 |
| 4.4 | Concluding Remarks and Future Scope | 77 |
| | References | 78 |
| 5 | An Overview of Computational-Based Strategies for Drug Repositioning | 81 |
| | <i>Shalu Verma, Nidhi Nainwal, Alka Singh, Gauree Kukreti and Kiran Dobhal</i> | |
| 5.1 | Introduction | 81 |
| 5.2 | Drug Repositioning | 82 |
| 5.2.1 | Computational Strategies for Drug Repositioning | 85 |
| 5.2.1.1 | IoT in Drug Repositioning | 85 |
| 5.2.1.2 | AI and ML in Drug Repositioning | 86 |
| 5.2.1.3 | Digital Twin in Drug Repurposing | 90 |
| 5.2.1.4 | Cloud Computing in Drug Repositioning | 91 |
| 5.2.1.5 | Big Data in Drug Repositioning | 91 |
| 5.3 | Challenges and Opportunities for Drug Repurposing | 93 |
| 5.4 | Conclusion | 94 |
| | References | 94 |
| 6 | Improving Performance With Feature Selection, Extraction, and Learning | 99 |
| | <i>Varsha K. Patil, Vrinda Shinde, Ritika Singh and Vipul Singh</i> | |
| 6.1 | Introduction | 99 |
| 6.2 | Feature Selection | 100 |
| 6.2.1 | Filter Methods | 101 |
| 6.2.1.1 | Procedure | 101 |
| 6.2.1.2 | Advantages | 103 |
| 6.2.1.3 | Disadvantages | 104 |
| 6.2.2 | Wrapper Method | 104 |
| 6.2.2.1 | Procedure | 105 |
| 6.2.2.2 | Advantages and Disadvantages | 106 |
| 6.2.2.3 | Forward Selection Algorithm | 106 |
| 6.2.2.4 | Backward Selection Algorithm | 107 |
| 6.2.3 | Embedded Method | 107 |
| 6.2.3.1 | Least Absolute Shrinkage and Selection Operator | 108 |
| 6.2.3.2 | Advantages | 109 |
| 6.2.3.3 | Disadvantages | 109 |

| | | |
|----------|--|------------|
| 6.3 | Feature Extraction | 110 |
| 6.3.1 | Principal Component Analysis | 110 |
| 6.3.1.1 | Procedure | 110 |
| 6.3.1.2 | Implementation | 111 |
| 6.3.1.3 | Advantages | 112 |
| 6.3.1.4 | Disadvantages | 113 |
| 6.3.2 | Linear Discriminant Analysis | 113 |
| 6.3.2.1 | Concept | 114 |
| 6.3.2.2 | Implementation | 114 |
| 6.3.2.3 | Advantages | 114 |
| 6.3.2.4 | Disadvantages | 115 |
| 6.4 | Feature Learning | 115 |
| 6.4.1 | Supervised Learning | 115 |
| 6.4.2 | Unsupervised Learning | 117 |
| 6.4.2.1 | Procedure | 118 |
| 6.4.2.2 | Advantages | 118 |
| 6.4.2.3 | Disadvantages | 119 |
| 6.4.3 | Deep Learning | 119 |
| 6.4.3.1 | Neural Network Architecture | 119 |
| 6.4.3.2 | Training Process | 121 |
| 6.4.3.3 | Advantages | 121 |
| 6.4.3.4 | Disadvantages | 122 |
| 6.4.4 | Machine Learning and Deep Learning | 122 |
| 6.5 | Future Research and Development | 123 |
| 6.6 | Future Scope | 124 |
| 6.7 | Conclusion | 125 |
| | References | 125 |
| 7 | Fusion of Phase and Local Features for CBIR | 129 |
| | <i>Pooja Sharma</i> | |
| 7.1 | Introduction | 129 |
| 7.2 | Overview of the Proposed System | 132 |
| 7.3 | Proposed Hybrid-Shape Descriptors | 132 |
| 7.3.1 | Global Feature Extraction Using ZMs | 133 |
| 7.3.1.1 | Recurrence Relation for Radial Polynomials $R_{pq}(r)$ | 134 |
| 7.3.1.2 | Recurrence Relation for Trigonometric Functions | 135 |
| 7.3.2 | Local Feature Extraction Using Hough Transform | 135 |
| 7.3.3 | Features Dimension | 135 |
| 7.3.4 | Effectiveness of the Proposed Descriptors | 137 |
| 7.4 | Similarity Measurement | 137 |
| 7.5 | Experimental Study and Performance Evaluation | 139 |
| 7.5.1 | Precision and Recall ($P - R$) | 139 |
| 7.5.2 | Database Construction | 140 |
| 7.5.3 | Experimental Study | 140 |

| | | |
|-----------|--|------------|
| 7.5.3.1 | Evaluation of Image Retrieval Performance on Subject Databases | 140 |
| 7.5.3.2 | Evaluation of Image Retrieval Performance on Geometric and Photometric Transformed Databases | 143 |
| 7.5.3.3 | Evaluation of Scalability and Time Complexity | 143 |
| 7.6 | Conclusions | 147 |
| | References | 148 |
| 8 | Trading Bot for Cryptocurrency Market Based on Smart Price Action Strategies | 151 |
| | <i>Divneet Singh Kapoor, Kiran Jot Singh, Anshoom Jain, Rhythm Chauhan, Khushal Thakur and Anshul Sharma</i> | |
| 8.1 | Introduction | 151 |
| 8.2 | Background | 154 |
| 8.3 | Proposed Framework | 156 |
| 8.4 | Results | 158 |
| 8.5 | Conclusion and Future Scope | 161 |
| | References | 161 |
| 9 | Comparative Evaluation and Prediction of Exoplanets Using Machine Learning Methods | 163 |
| | <i>Divneet Singh Kapoor, Kiran Jot Singh, Ashirvad Singh, Benarji Mulakala, Karan Singh, Prashant, Ramanjeet Singh and Shubham Mahajan</i> | |
| 9.1 | Introduction | 164 |
| 9.2 | Background | 167 |
| 9.3 | Proposed Framework | 169 |
| 9.4 | Results | 171 |
| 9.5 | Conclusion and Future Scope | 182 |
| | References | 183 |
| 10 | The Risk of Using Failure Rate With the Help of MTTF and MTBF to Calculate Reliability | 185 |
| | <i>Harpreet Kaur and Shiv Kumar Sharma</i> | |
| 10.1 | Introduction | 185 |
| 10.2 | Failure | 186 |
| 10.2.1 | Failure Rate | 187 |
| 10.2.2 | Mean Time Between Failure | 187 |
| 10.2.3 | Mean Time to Failure | 187 |
| 10.2.4 | Reliability | 187 |
| 10.2.5 | Fault Tree Analysis | 189 |
| 10.2.6 | Fault Tree Symbols Logic Entrance | 190 |
| 10.2.6.1 | OR-Gate | 190 |
| 10.2.6.2 | AND-Gate | 190 |
| 10.2.7 | Regulations for Fault Tree Structure | 190 |
| 10.2.7.1 | Illustrate the Fault Actions | 190 |
| 10.2.7.2 | Estimate the Fault Events | 190 |
| 10.2.7.3 | Inclusive the Gates | 191 |

| | | |
|-----------|--|------------|
| 10.3 | Conclusion | 191 |
| | References | 192 |
| 11 | A Detailed Description on Various Techniques of Edge Detection Algorithms | 193 |
| | <i>Pritha A. and G. Fathima</i> | |
| 11.1 | Introduction | 193 |
| 11.2 | Edge Detection Techniques | 194 |
| 11.2.1 | Steps in Edge Detection | 194 |
| 11.2.2 | Gradient-Based Techniques | 194 |
| 11.2.2.1 | Sobel Edge Detected Operator | 194 |
| 11.2.2.2 | Prewitt Edge Detected Operator | 197 |
| 11.2.2.3 | Robert Cross Edge Detection Operator | 198 |
| 11.2.3 | Gaussian Based Technique | 200 |
| 11.2.3.1 | Canny Edge Detector | 200 |
| 11.2.3.2 | Canny Operator Architecture | 203 |
| 11.3 | Experimental Results | 203 |
| 11.4 | Comparative Results | 203 |
| 11.5 | Conclusion | 203 |
| 11.6 | Future Work | 204 |
| | References | 205 |
| 12 | Advancement of ML in Smart House | 207 |
| | <i>Gokula Udhayan V., K. Mahaeshwari and N. Vinoth Kumar</i> | |
| 12.1 | Objective | 207 |
| 12.2 | Introduction | 207 |
| 12.3 | Smart House System With IoT | 208 |
| 12.3.1 | Elements of Smart Home | 208 |
| 12.3.2 | Smart Home Application Framework | 209 |
| 12.3.2.1 | Cloud Computing in IoT | 209 |
| 12.3.2.2 | Smart House System | 209 |
| 12.3.3 | LPG Detecting System | 210 |
| 12.3.3.1 | Materials Description | 210 |
| 12.3.3.2 | Circuit Diagram | 211 |
| 12.3.3.3 | Power Consumption | 212 |
| 12.3.3.4 | Components Required | 212 |
| 12.3.4 | Materials Description | 213 |
| 12.3.4.1 | NodeMCU 8266 | 213 |
| 12.3.5 | Online Switch | 215 |
| 12.3.5.1 | Components Required | 215 |
| 12.3.5.2 | Circuit Diagram | 216 |
| 12.3.5.3 | Materials Description | 216 |
| 12.3.5.4 | Projects in Smart House Systems | 217 |
| 12.3.6 | Introducing Image Processing | 218 |
| 12.3.6.1 | Image Processing | 218 |
| 12.3.6.2 | Machine Learning in Automation | 219 |

| | | |
|-----------|---|------------|
| 12.3.6.3 | Online Switch | 220 |
| 12.3.6.4 | Machine Learning Module | 221 |
| 12.3.7 | Plants Health Monitoring | 221 |
| 12.3.7.1 | Components Required | 221 |
| 12.3.7.2 | Working of the System | 221 |
| 12.4 | Future Scope | 223 |
| 12.5 | Conclusion | 223 |
| | References | 224 |
| 13 | Multi-Robot Navigation: A Biologically Inspired Framework | 225 |
| | <i>Imran Mir and Faiza Gul</i> | |
| 13.1 | Introduction | 225 |
| 13.1.1 | Motivation | 226 |
| 13.2 | Optimization Algorithms | 226 |
| 13.2.1 | Mathematical Formulation | 227 |
| 13.2.2 | Gradient-Based Approaches | 228 |
| 13.2.3 | Gradient-Free Algorithm | 229 |
| 13.2.4 | Nature-Inspired Optimization Algorithms | 229 |
| 13.2.5 | Genetic Algorithms | 230 |
| 13.2.6 | Particle Swarm Optimization | 230 |
| 13.2.7 | Ant Colony Optimization | 231 |
| 13.2.8 | Grey Wolf Algorithm | 231 |
| 13.2.9 | Arithmetic Algorithm | 232 |
| 13.2.10 | Aquila Optimization Algorithm | 233 |
| 13.2.11 | Different Algorithms | 236 |
| 13.3 | Algorithms and Self-Organization | 236 |
| 13.3.1 | Algorithmic Attributes | 236 |
| 13.3.2 | Comparison With Classical Optimization Techniques | 236 |
| 13.3.3 | Self-Organized Systems | 237 |
| 13.4 | Future Research Directions | 238 |
| 13.5 | Conclusion | 239 |
| | References | 239 |
| 14 | Bidirectional LSTM for Heart Arrhythmia Detection | 243 |
| | <i>Nikhil M. Agrawal, H. D. Bhanu Cheitanya, Abhishek Kumar Rai and Shubham Mahajan</i> | |
| 14.1 | Introduction | 243 |
| 14.2 | About the Dataset | 245 |
| 14.3 | Flow of the Model | 246 |
| 14.4 | Results | 248 |
| 14.5 | Conclusion | 248 |
| | References | 250 |
| 15 | Study on Content-Based Image Retrieval | 253 |
| | <i>Thanga Subha Devi M., R. Suji Pramila and Tibbie Pon Symon</i> | |
| 15.1 | Introduction | 254 |

| | | |
|-----------|---|------------|
| 15.2 | Related Works | 256 |
| 15.2.1 | Conventional-Indexing Techniques | 256 |
| 15.2.2 | Dimensionality's Curse | 257 |
| 15.2.2.1 | Parallel Architecture | 257 |
| 15.2.2.2 | Hashing | 257 |
| 15.2.2.3 | Reduction of Size | 258 |
| 15.2.2.4 | Bag-of-Features | 258 |
| 15.3 | Extraction of Features | 261 |
| 15.3.1 | Color | 261 |
| 15.3.1.1 | Color Space | 261 |
| 15.3.1.2 | Method of Representation | 263 |
| 15.3.2 | Texture | 264 |
| 15.3.2.1 | Method of Depiction | 264 |
| 15.3.3 | Shape | 266 |
| 15.3.3.1 | Methods of Representation | 266 |
| 15.4 | User Interactions for CBIR System | 266 |
| 15.4.1 | Query Description | 267 |
| 15.4.2 | Result Visualization | 267 |
| 15.4.2.1 | Performance Metrics | 268 |
| 15.4.3 | Relevance Feedback | 269 |
| 15.5 | Conclusions | 269 |
| | References | 270 |
| 16 | Machine Learning and Angiogenesis in Cancer | 273 |
| | <i>Dharambir Kashyap, Riya Sharma, Neelam Goel and Vivek Kumar Garg</i> | |
| 16.1 | Introduction | 273 |
| 16.2 | History of Angiogenesis Discovery | 274 |
| 16.3 | Overview of Angiogenesis | 274 |
| 16.4 | Angiogenesis in Carcinogenesis | 275 |
| 16.5 | Molecular Mechanisms of Angiogenesis Formation | 276 |
| 16.6 | Angiogenesis as a Target in Cancer Therapy | 276 |
| 16.7 | Machine Learning Approaches in Angiogenesis | 277 |
| 16.8 | Conclusion | 278 |
| | References | 279 |
| 17 | Handwritten Image Enhancement Based on Neutrosopic-Fuzzy and K-Mean Clustering | 283 |
| | <i>Jaspreet Kaur, Divya Gupta, Simarjeet Kaur and Amrinder Singh</i> | |
| 17.1 | Introduction | 284 |
| 17.1.1 | Image Acquisition | 284 |
| 17.1.2 | Image Segmentation | 285 |
| 17.1.3 | Image Filtering | 285 |
| 17.1.4 | Image Enhancement | 285 |
| 17.1.5 | Clustering | 285 |
| 17.1.6 | Image Restoration | 285 |
| 17.1.7 | Data Compression for Image | 286 |

| | | |
|-----------|--|------------|
| 17.1.8 | Color Image Processing | 286 |
| 17.2 | Application of Image Processing | 286 |
| 17.2.1 | In Healthcare | 286 |
| 17.2.2 | In Robotics | 286 |
| 17.2.3 | In Defence | 286 |
| 17.2.4 | In Agriculture | 286 |
| 17.2.5 | In Manufacturing | 287 |
| 17.2.6 | In Entertainment | 287 |
| 17.2.7 | Object Recognition | 287 |
| 17.3 | Enhancement of Handwritten Document | 287 |
| 17.3.1 | Local Thresholding Technique | 287 |
| 17.4 | Clustering Techniques | 288 |
| 17.4.1 | K-Means Clustering Technique | 288 |
| 17.4.2 | Combination of Neutrosopic and Fuzzy Type 1 Technique | 289 |
| 17.5 | Performance Parameters | 290 |
| 17.5.1 | Mean Square Error | 290 |
| 17.5.2 | Root Mean Square Error | 291 |
| 17.5.3 | Peak Signal to Noise Ratio | 291 |
| 17.5.4 | Normalized Coefficient | 291 |
| 17.5.5 | Distance Reciprocal Distortion Metric | 292 |
| 17.6 | Results and Discussion | 293 |
| 17.6.1 | Peak Signal-to-Noise Ratio | 293 |
| 17.6.2 | Normalized Coefficient | 293 |
| 17.6.3 | Distance Reciprocal Distortion Metric | 294 |
| 17.7 | Conclusion | 295 |
| | References | 295 |
| 18 | A Texture Classification System Based on an Adaptive Histogram Equalized Shearlet Transform | 299 |
| | <i>K. Gopalakrishnan, V. Karthikeyan and P.T. Vanathi</i> | |
| 18.1 | Introduction | 299 |
| 18.1.1 | Texture Analysis and Texture Classification | 301 |
| 18.1.2 | Texture Analysis Methods | 302 |
| 18.2 | Literature Survey | 303 |
| 18.3 | Materials and Methods | 305 |
| 18.3.1 | Continuous Shearlet | 305 |
| 18.3.2 | Discrete Shearlet | 306 |
| 18.3.3 | Shearlet Decomposition | 307 |
| 18.3.4 | Feature Extraction | 307 |
| 18.3.5 | Classifiers | 309 |
| 18.3.5.1 | Minimum Distance Classifier | 309 |
| 18.3.5.2 | SVM | 309 |
| 18.4 | Proposed Methodology | 309 |
| 18.4.1 | Adaptive Histogram Equalization Method | 310 |
| 18.4.2 | AHE Algorithm | 310 |
| 18.5 | Result and Discussion | 311 |

| | | |
|--------------|---|------------|
| 18.5.1 | Experimental Dataset | 311 |
| 18.5.2 | Experiment 1 | 312 |
| 18.5.3 | Experiment 2 | 317 |
| 18.6 | Conclusion | 320 |
| | References | 320 |
| 19 | A Thyroid Nodule Detection Using L1-Norm Inception Deep Neural Network | 323 |
| | <i>Saranya G.</i> | |
| 19.1 | Introduction | 323 |
| 19.2 | Related Work | 324 |
| 19.3 | Methodology | 325 |
| 19.3.1 | Preprocessing | 326 |
| 19.3.2 | Noise Removal With Lee Filter | 326 |
| 19.3.3 | Hybrid Pyramid Fusion Algorithm | 327 |
| 19.3.4 | L1-Norm Inception Deep Neural Network Classification | 327 |
| 19.4 | Results and Discussion | 329 |
| 19.4.1 | Classification Performance Evaluation | 330 |
| 19.4.2 | Recall | 332 |
| 19.4.3 | Precision | 333 |
| 19.4.4 | Accuracy | 334 |
| 19.4.5 | Specificity | 334 |
| 19.4.6 | F1 Score | 334 |
| 19.5 | Conclusion | 336 |
| | References | 337 |
| Index | | 339 |

Preface

Currently, the use of digital images and videos has extended to different fields, such as surveillance, manufacturing, medicine, agriculture, machine and robot vision, pattern recognition, etc. They are easy to obtain from various environments, and it is necessary to recognize the objects contained in the scenes. To achieve this goal, several computational approaches have been developed; however, considering the technological advances in problems, such as image size, noise, illumination and security, it is necessary to develop new methodologies and to improve the classical algorithms.

On the other hand, computer vision and image processing systems should be able to automatically extract the desired features for a particular task. Computational Intelligence (CI) approaches are alternative solutions for automatic computer vision and image processing systems; they include the use of tools, such as machine learning and soft computing. Researchers from all over the world are working hard to create new algorithms that combine the methods provided by CI approaches to solve the problems of image processing and computer vision. This book provides high-quality research work that addresses broad challenges in both theoretical and application aspects of soft computing and machine learning in image processing and computer vision.

This resource is useful for a variety of readers, with three specific audiences in mind. One of these target audiences is university students (undergraduate, graduate, or post-graduate) who are learning about communication, automation, and power engineering. The second group includes those who are beginning a career in research and innovation. The third target audience consists of researchers and practitioners who lack an in-depth background in automation and engineering but want to rapidly acquire one and begin using it in their product development or platform.

This book comprises 19 chapters. Chapter 1 and Chapter 2 discuss the advancement in diagnostic and therapeutic techniques for ischemic stroke and object detection and tracking face detection and recognition. The third chapter discusses the future of medicine, namely 3D printing organs. Comparative evaluation of machine learning algorithms for bank fraud detection, an overview of computational-based strategies for drug repositioning and improving performance with feature selection, extraction, and learning are detailed in Chapters 4, 5, and 6. The proposed method is capable of retrieving transformed images as well, i.e., the proposed system is robust at photometric and geometric transformations, which is covered in detail in Chapter 7.

Chapter 8, 9, 10, and 11 respectively deal with the concept of trading for the cryptocurrency market based on smart price action strategies, comparative evaluation, and prediction of exoplanets using machine learning methods; the risk of using failure rate with the help of MTTF and MTBF to calculate reliability; and a detailed description of various techniques using edge detection algorithms.

Chapter 12 explores the logic and advancement of ML in smart houses. Chapter 13 highlights the strengths and limitations of swarm intelligence and computation. As a speedy reference for readers, this section identifies probable future directions that can address unresolved issues. Chapter 14 shows how to use bidirectional LSTM for heart arrhythmia detection. A comprehensive study on content-based, image-retrieval techniques for feature extraction is detailed in Chapter 15, which Chapter 16 describes the angiogenesis, its role in cancer and mechanism, and machine learning approaches to understanding angiogenesis. Chapter 17, 18, and 19 pertain to handwritten image enhancement based on neutrosopic-fuzzy and K-Mean clustering, a texture classification system based on an adaptive histogram, and thyroid nodule detection using an L1-Norm inception, deep neural network.

We are deeply grateful to everyone who helped with this book and greatly appreciate the dedicated support and valuable assistance rendered by Martin Scrivener and the Scrivener Publishing team during its publication.

The Editors
April 2024

Advancement in Diagnostic and Therapeutic Techniques for Ischemic Stroke

Mukul Jain^{1,2}, Divya Patil², Shubham Gupta³ and Shubham Mahajan^{4,5,6*}

¹Cell & Developmental Biology Lab, Research and Development Cell, Parul University, Vadodara, Gujarat, India

²Department of Life Sciences, Parul Institute of Applied Sciences, Parul University, Vadodara, Gujarat, India

³Department of Paramedical and Health Sciences, Faculty of Medicine, Parul University, Vadodara, Gujarat, India

⁴School of Engineering, Ajeenkya D Y Patil University, Pune, Maharashtra, (iNurture Education Solutions Pvt. Ltd., Bangalore), Pune, Maharashtra, India

⁵University Center for Research & Development (UCRD), Chandigarh University, Mohali, India

⁶Hourani Center for Applied Scientific Research, AI-Ahilyaya Amman University, Amman, Jordan

Abstract

Ischemic stroke is a cerebrovascular disease that is typically brought on by a disruption in the blood flow to the brain; it accounts for more than 80% of all strokes. 1.8 million neurons are thought to die per minute. The burden of stroke in people younger than 65 years has increased over the last decades, it has increased worldwide by 25% among adults aged 20 to 64 years. According to reports, both men and women can experience stroke symptoms, in this case women are more prone to have nontraditional symptoms of stroke like dizziness, lack of consciousness, slurred speech. In comparison to Western Europe, America, Australia, and similar to Eastern Europe, Asia has a higher stroke fatality rate. Acute management of stroke requires fast and efficient screening, imaging and modality. Better clinical outcomes can be attained through early detection and treatment of stroke. Stroke imaging techniques are computed tomography (CT) scans and magnetic resonance imaging (MRI). MRI is more preferred because it gives detailed and exact result of damage. Antithrombotic and neuroprotective therapies are the mainstays of conventional medicine, although their use is still constrained due to their poor safety. Utilizing nanomedicines is an additional option since they can boost therapeutic benefit and adverse effect reduction, achieve effective medicine collection at the target site, and improve pharmacokinetic behavior of pharmaceuticals *in vivo*. We have comprehensively described ischemic stroke, its epidemiology, advanced artificial intelligence-based diagnostic tools and its treatment therapies.

Keywords: Ischemic stroke, computed tomography, MRI, artificial intelligence, diagnostic tools, PET, EEG, nanomedicine

*Corresponding author: mahajanshubham2232579@gmail.com

1.1 Introduction

Stroke is a fatal and disabling illness that affects more than 15 million individuals annually worldwide. It is an ageing disease that primarily affects persons over the age of 65 years [1, 2]. In the US, ischemic strokes, which are caused by a decrease in brain blood circulation, account for 87% of all cases [2]. According to a report released by WHO in 2016, strokes are the second most frequent cause of impairment in the population today worldwide (Figure 1.1). With the passing of each decade during the previous 40 years, it has been revealed that the number of stroke cases multiplied [11]. Both the incidence and prognosis of stroke are influenced by gender; nevertheless, overall, women have a higher stroke prevalence than men do due to aging-related increases in stroke risk and longer average lifespans for women [3]. Basic stroke classifications include hemorrhagic, transient ischemic attack, and

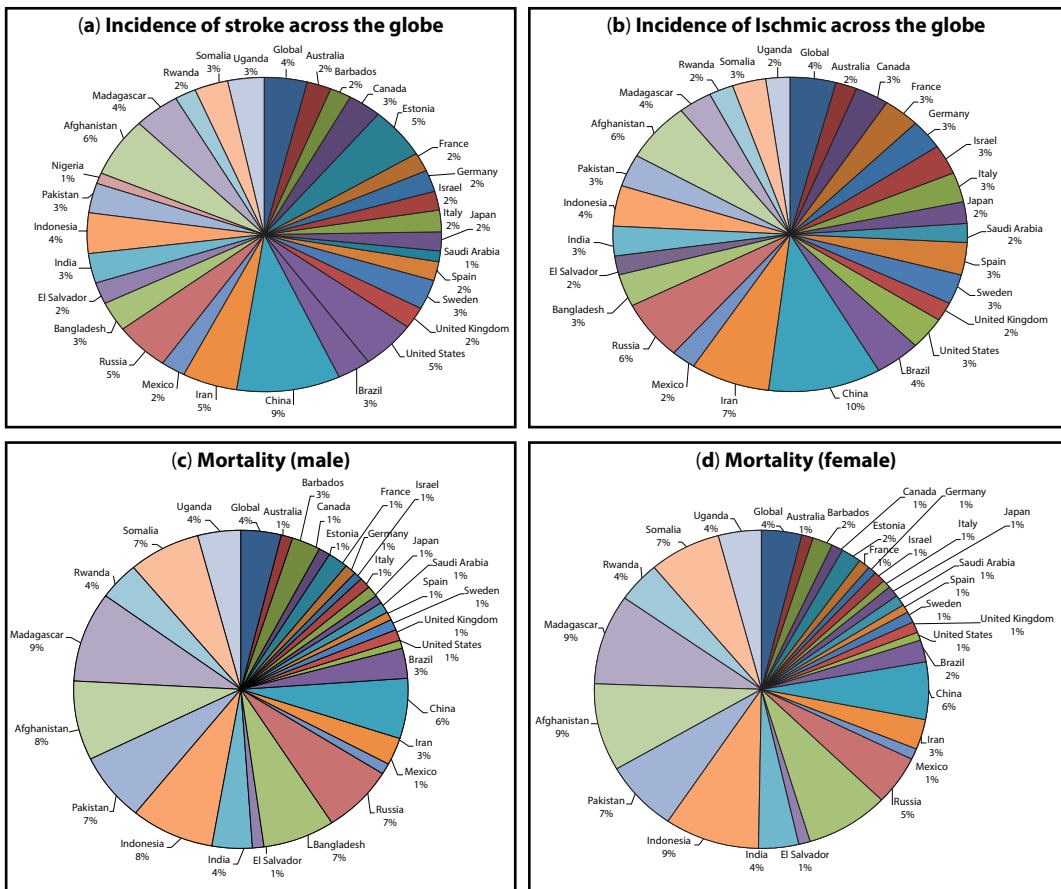


Figure 1.1 The data represent country wise occurrence of stroke and mortality rate in male and female across the world. (a) Incidence of stroke worldwide, in which china has higher percentage rate that is 9% and lower rate in Saudi Arabia that is 1%. (b) Prevalence of ischemic stroke across the world covering 28 countries, the higher incidence of ischemic stroke is 10% and low rate is 2%. (c) The percentage of mortality rate of stroke in male across the globe is 4%, high mortality rate is reported in Madagascar that is 9%. (d) The percentage of mortality rate in female across the world, high mortality is noted in Madgascar, Afghanistan, and Indonesia that is 9%.

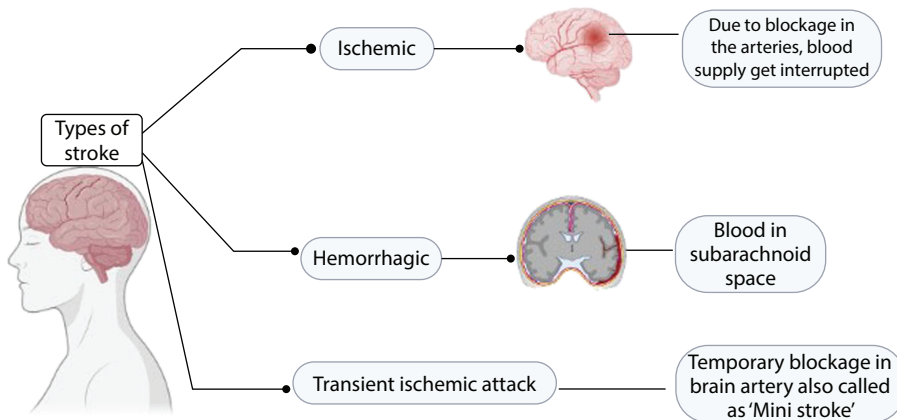


Figure 1.2 It demonstrates the different types of stroke occurrence and how it causes in the brain and disturbs the brain function.

ischemic strokes (Figure 1.2). Nearly 80% of strokes are ischemic, while various populations experience hemorrhagic and ischemic strokes more frequently in varied proportions [4]. The following categories—etiologic subtypes—have been used to further categorize ischemic strokes: cardioembolic, atherosclerosis, lacunar, other particular causes (dissections, vasculitis, specific hereditary illnesses, etc.), and strokes with no known etiology [5]. Prior to the main stroke episode, individuals always have ministrokes, commonly referred to as transient ischemic attacks (TIA). The majority of published research relies on MRI and CT scan pictures to categorize strokes, which is a costly method of early stroke detection. CT and MRI are employed in the majority of investigations that identify strokes. These days, noninvasive methods are becoming more and more common. One such method is the electroencephalograph (EEG), which is also a cheap or free method. The following issues have impeded the advancement of novel therapeutics for ischemic stroke and numerous other illnesses of the central nervous system (CNS): blood–brain barrier (BBB) prevents most CNS drugs from reaching the brain parenchyma effectively, which makes it difficult to treat or save areas of the brain that haven't yet been completely affected; (2) many drugs have poor stability or toxicity after systemic and/or oral administration; (3) the pathophysiology of the disease is not well understood; and (4) it is challenging to translate positive results from preclinical studies to the clinic [6]. One of the key problems in the treatment of stroke is the blood brain barrier. In order to transport enough medicine to the brain tissue, liposomes must be able to cross the BBB and it is ideal for them to stay in the bloodstream for a long time [7]. New stroke diagnostic methods have been created thanks to nanotechnology and artificial nanomaterials. Identifying the biochemical and pathophysiological causes of stroke may be made easier with the help of this technology [8]. Due to their distinct fluorescence characteristics, which enable high spatiotemporal accuracy at biologically relevant concentrations, optical CNT-based biosensors exhibit considerable potential [9, 10]. With the development of nanotechnology, it is now possible to carry drugs to the brain and, more precisely, the area that is ischemia, more efficiently [8]. The FDA has only approved one therapeutic drug—recombinant tissue plasminogen activator (tPA)—for the treatment of ischemic stroke, and its use is constrained by its limited therapeutic window, quick drug elimination, and potential for hemorrhagic transformation [138]. There is no particular

cure in medical science to deal with strokes; therefore, early identification is the key to deal with strokes. The early identification can inhibit the disabilities, loss of deaths, and other brain-related severe problems [12].

1.2 Diagnostic Tools of Ischemic Stroke

1.2.1 Preimaging

Patients with acute neurological conditions require quick neuroimaging. American Stroke Association recommendations recommend that the only prior inquiry is an actual capillary blood glucose, which is retrieved from paramedics. What is an intravenous cannula for contrast or perfusion imaging is frequently necessary sequences, enabling the simultaneous collection of a blood panel. This often includes a coagulation screen, a renal function test, and an infection test if the patient uses anticoagulants. Though many departments of radiology demand a current renal function prior to providing contrast [10].

1.2.2 Imaging

1.2.2.1 *Computed Tomography Scan*

Neuroimaging in the setting of a hyperacute severe stroke is still primarily based on CT. A noncontrast CT scan of head is rapid, delicate, and cost-effective excluding cerebral bleeding, which is typically sufficient to make judgments on thrombolysis. Due to widespread availability and significantly shorter turnaround times, CT perfusion investigations are extraeffective in the accident scenario to detect and identify stroke patients who can profit from thrombolytic therapy and vascular blood flow [134, 135] CT perfusion sequences can evaluate a variety of brain perfusion is frequently performed using artificial intelligence, like MIstar (Apollo Medical Imaging Technology) or iSchemaView's Rapid Processing of Perfusion and Diffusion (RAPID) CT perfusion. The contrast bolus-tracking approach known as CT perfusion can be used with almost any multidetector CT scanner that is now in use in emergency rooms all around the world [131, 132]. A crucial factor in determining the dangers and possible benefits of reperfusion treatments, ideal CT perfusion values and thresholds that characterize irreversible infarction have not received enough attention in research [133]. These technologies make interpretation easier by ensuring the use of validated thresholds and enhancing interobserver reproducibility [10]. The sensitivity of the CT signals is between 40% and 60% within the first 3 hours following the beginning of symptoms, and their positive, negative predictive values and specificity are correspondingly 96%, 27%, and 85%. About 45 minutes after the onset of ischemia is when the hypodensity can be first detected. The severity of a middle cerebral artery (MCA) stroke can be determined by a noncontrast head CT scan utilizing the Alberta Stroke Program Early CT Score (ASPECTS). According to current recommendations, the time to CT and the reporting of preliminary findings should be under 20 minutes [15]. The overall pooled susceptibility for the CT perfusion method was 55.7%, while the specificity was 92%, based on a meta-analysis done in 2015. According to a 2017 study, CT perfusion scanning has a specificity and sensitivity of 92% and 82%, accordingly. This investigation emphasized the dominance of CT perfusion study over noncontrast CT (NCCT) brain, arguing that while NCCT brain

can typically identify ischemic infarct, it is of little usefulness in identifying the premature acute ischemic infarction (24-hour window following the beginning of symptoms) and is affected by the seriousness and size of the infarct. The advantage of CT perfusion is that it can identify ischemic stroke symptoms early that noncontrast CT scans cannot [136].

1.2.2.2 *Magnetic Resonance Imaging*

A more accurate and widely used technique is the MRI stroke protocol for the diagnosis of acute brain ischemia alterations. For locating the infarct core, MRI is still the gold standard [13]. The way to determine the acute ischemic core volume is unquestionably MRI with DWI (Diffusion weighted imaging) and T2 FLAIR (T2 Fluid attenuated inversion recovery) sequences; their sensitivity and specificity. When water molecules move from the extracellular to the intracellular space at the time of Na⁺/K⁺ ATPase, which happens at this stage of cytotoxic edema, DWI can detect hyperacute ischemic alterations [14]. Due to the restricted motion of the water molecules stuck in the cell, DWI can identify cytotoxic edema [20]. Standardized stroke MRI protocols take about 10 minutes in facilities that have used MRI as the primary diagnostic imaging technique for years. With the aid of echo planar imaging at 3 Tesla, this time might be cut down to 6 minutes [16–18]. A stroke that happened during the last 4.5 hours and might benefit from thrombolysis is identified by MRI [19]. Patients with incapacitating acute ischemic stroke (arbitrary definition: NIHSS>6) due to imaging-proven anterior circulation major vessel blockage for up to 6 hours and posterior circulation (basilar or posterior cerebral artery) 24 hours following the occurrence of symptoms, large-vessel occlusion. Another technique that might be utilized to assess suspected large vessel occlusion LVO and its localization by MRI. In MR angiography (MRA), there are two technological options: native or unenhanced MRA, which predominantly uses the time of flight (TOF) approach, and contrast enhanced MRA (CEMRA), which uses an intravenous gadolinium-based contrast agent (GBCA) [21]. CEMRA is a method that uses T1-weighted spoiled gradient-echo sequences after GBCA is injected intravenously. You can collect single-phase or multiphasic data. For MIP and VRT 3D reconstructions, the original data may once again be utilized. The previous restrictions on various flow artefacts are removed by CEMRA [22]. A complete MRI scan including CEMRA may require about 15 minutes. In AIS with LVO, it is estimated that in the worst-case scenario, every minute loses 1.9 million neurons and 12 km of myelinated fibers, and that an hour of inefficiency costs 120 million neurons, 714 km of lost myelinated fibers, and 3.6 years of accelerated ageing [23]. NECT for hemorrhage detection, ASPECTS assessment, and CTA for occlusion detection, that is all required in the acute context, particularly in the early time window. Additionally, MRI is more sensitive than NECT at detecting subacute or chronic intracerebral hemorrhage as well as microhemorrhages. Despite the fact that current guidelines and recommendations support CTP or MRI for the assessment of the ischemic core in the late and unidentified time frame [24, 25]. It is crucial to emphasize that CTP and MRI play a vital role in research and in understanding the pathophysiological process of stroke and its therapy [14]. Instead of allowing for direct observation of the arteries, MR perfusion imaging depends on the detection of tracer chemicals inside blood. The DAWN and DEFUSE 3 trials were two important stroke studies that altered the standard of care for individuals with large-vessel occlusion stroke who show within 6 to 24 hours of the onset of symptoms (determined as the “time last seen well” [TLSW]), allowing for the signs of endovascular therapy for

this extended time window. It is crucial to differentiate between triage that is done to find individuals that can benefit from therapy (the right use of imaging), and triage that is done to find patients who might have favorable results than others (an inappropriate goal in the context of individual medical care). Patients chosen based on the best CTP parameters tend to have better clinical outcomes, but such choice may boost statistics generally at the expense of neglecting many patients who would benefit [137].

1.2.2.3 *Electromyography*

The most often utilized method for learning about how muscles are controlled by their neuromuscular system is electromyography (EMG) [26, 27]. EMG is successfully used in clinics for surgical procedures and diagnostic support [28]. EMG has recently been investigated as an alternative brain-computer for detecting movement intention using brain-computer interaction (BCI) [29]. Additionally, investigations on the viability of using EMG for human and muscle-computer interfaces have been conducted [30, 31]. In order to quantify muscle contraction velocity and analyze motor neurons and innervation zones, frequency-domain and time-domain analysis are most frequently utilized for surface EMG analysis [39]. The ideal feature vector has been created using time-domain features such root mean square (RMS), waveform length (WL) and Willison amplitude (WAMP) and waveform length (WL) [32, 33]. The most useful and often utilised frequency-domain parameters for determining muscle fatigue are median frequency (MDF) and mean frequency (MNF) [33]. The frequency-domain power spectrum technique, however, demonstrated more accuracy in determining muscle wear and tear [34].

1.2.2.4 *Electroencephalography (EEG)*

EEG, which records the electrical activity of the brain, has been investigated as a stroke diagnostic and predictive tool [35, 36]. Within the first three months following a stroke, the power spectrum starts to return to normal, but quantitative EEG (qEEG) can still reveal abnormalities that last past the threshold of excellent motor recovery, such as poor symmetry [37]. First time the brain symmetry measure was used to reliably identify early brain ischemia was during carotid surgery [38]. There is a need for an EEG device that is affordable, straightforward to set up, and simple to understand. Consumer wireless EEG systems that satisfy these demands have been made possible by technological advancements. One sort of wearable consumer EEG system that is commercially available and has been contrasted with medical EEG devices is The Muse by InteraXon Inc [39]. In order to evaluate the value of employing EEG in the hyperacute phase of stroke, future research will screen patients sooner, such as in the emergency room or in the ambulance [40].

1.2.2.5 *Positron Emission Tomography (PET)*

The first to show that the penumbra exists in people among the different stroke imaging modalities was PET in 1980 [41]. The “gold standard” for assessing early stroke pathogenesis is PET [42]. The fact that PET provides semiquantitative or quantitative hemodynamic data is one of its other key advantages [43]. Numerous PET imaging methods, such as multitracer PET with 15O, PET with flumazenil (FMZ), and PET with fluoromisonidazole, are

available (FMISO). Each approach has particular advantages and disadvantages. The penumbra is identified as tissue with “misery perfusion” (lower CBF but maintained CMRO₂ due to higher OEF) by multitracer PET, which produces quantitative maps of CBF, cerebral blood volume (CBV), CMRO₂, and CMRglu [44]. The issue with multitracer PET was the substantial variation in penumbral CBF values (from 4.8 to 14.1 in one analysis and from 7 ml/100 g/min to 22 ml/100 g/min in another). This illustrates how OEF is an unreliable indicator of tissue viability and how data from a single point in time can be perplexing when the overall trend is not known. Due to this, a marker that can recognize irreversibly damaged tissue independent of the length of time since the stroke began or changes in CBF over time is required [44]. PET with FMZ occurred as a result [45]. As it is diminished in all metabolically active tissue (except from the infarcted core), FMISO identifies the penumbra by designating hypoxic tissue. Oxygenated tissue is able to reoxidize the metabolite to its original form, but hypoxic tissue is unable to do so. The tissue at risk is then marked by the metabolite’s binding to intracellular molecules [46]. Since some tissue maintains oxygenation in regions of low CBF by raising OEF and since some tissue has a lower baseline CBF and metabolic rate, hypoxia may be a more accurate predictor of tissue at risk than CBF (such as white matter) [46]. Theoretically, the fact that animals have a considerably lower white to grey matter ratio than humans is one reason why neuroprotectants that are effective in animal models cannot be translated to humans. This method would enable testing of white matter neuroprotectants because FMISO can image ischemic white matter [46]. However, the utility of PET in clinics is constrained by technical requirements and the brief half-life of ¹⁵O radiotracers [41].

1.3 Artificial Intelligence–Based Diagnostic Tools

There are numerous uses for artificial intelligence technologies in acute stroke imaging, with ischemic and hemorrhagic stroke types. Infarct or hemorrhage identification, segmentation, classification, major vascular occlusion detection, Alberta Stroke Program Early CT Score grading, prognostication, and other components of the stroke therapy paradigm can all be aided by artificial intelligence. Particularly, cutting-edge AI methods like convolutional neural networks hold promise for effectively and accurately carrying out these imaging-based activities [47]. An input, one or more hidden layers, and an output are the components of artificial neural networks (ANNs), a kind of deep learning (DL) that imitates biological neurons. An input, one or more hidden layers, and an output are the components of artificial neural networks (ANNs), a kind of deep learning (DL) that imitates biological neurons [47]. Due to the limited window of therapeutic efficacy, early diagnosis of ischemia infarction is crucial when considering patients as possible candidates for thrombolysis [47]. Identification of patients who might benefit from mechanical thrombectomy depends on the diagnosis of LVO. On NCCT, an SVM algorithm had a high sensitivity (97.5%) for detecting the MCA dot sign in patients with acute stroke [48]. AUC of 86.3% (95% CI, 0.83–0.90; $P=0.001$), intraclass correlation coefficient (ICC) of 84.1% (95% CI, 0.81–0.86; $P=0.001$), and accuracy of 86% were achieved by CNN-based commercial software, Viz-AI Algorithm v3.04 in detecting proximal LVO, and high sensitivity and specificity (82% and 94%, respectively) were achieved by Viz-AI [49, 50]. GoogLeNet with augmented data in a pretrained network was the most accurate (AUC 14 1.0; sensitivity and specificity 14 100%)

compared to the highest performing augmented, untrained AlexNet (AUC 14 0.95; sensitivity 14 100%; and specificity 14 80%), according to a study using two 2D convolutional neural networks, GoogLeNet and AlexNet, to detect basal ganglia hemorrhage [51]. More than 30,000 NCCTs from various hospitals in India were investigated by one of the biggest cohorts for the identification and categorization of ICH utilizing DL algorithms [52]. Another study was able to identify ICH and reprioritize studies as “stat” (defined as a positive ICH study) versus “routine” utilizing a fully 3D CNN and a sizable patient population [53]. Time to detection decreased from 512 to 19 minutes when the algorithm was incorporated into the radiologist’s workflow [47].

1.4 Blood-Based Protein Biomarker for Stroke

The use of radiological pictures for stroke diagnosis and distinction has been hampered by advancements in the field of neuroimaging, as well as possible drawbacks such their time-consuming nature, high equipment costs, limited availability, and variability in the analysis of radiological images [54]. It is very difficult to find ideal biomarkers that are engaged in cellular processes specific to ischemic stroke. Protein concentrations that are typically found in large concentrations in the brain not in the blood are obvious individuals [139]. Blood biomarkers may provide a dependable, quick, and affordable technique to distinguish between IS and HS. The choice of the best therapy options for patients who have suffered an acute stroke may be aided by specific biomarker signatures. To effectively and efficiently identify IS from HS in acute settings for better treatment measures, a blood-based biomarker method with high sensitivity and specificity is needed [55].

1.5 Markers for Endothelial Damage

The probable function of the Apo C-I and Apo C-III proteins in detecting HS and IS was discussed in a study by Allard *et al.* (2004) [56]. The relative fluorescence units were used to express the levels of Apo C-I and Apo C-III (RFU). In order to discriminate between 15 IS and 16 HS patients, Apo C-I was found to have a susceptibility of 94% and specificity of 73% with the cutoff point at 60 RFU, whereas Apo C-III was reported to have a sensitivity of 94% and specificity of 87% with a cutoff point at 36 RFU. Within 6 hours of the beginning of symptoms, both Apo C-I and Apo C-III levels were shown to be higher in IS than HS. A few years later, Lopez *et al.* (2012) [57] used a Selective Reaction Monitoring (SRM)-based test to evaluate nine apolipoproteins (Apo A-I, Apo A-II, Apo B, Apo C-I, Apo C-II, Apo C-III, Apo D, Apo E, Apo H) for detecting IS and HS patients within the first week of symptom onset. They discovered that Apo C-III (individually) identified between IS and HS with an area beneath the curve (AUC) of 0.85 out of the nine apolipoproteins assessed. Kim *et al.* (2010) examined a panel of four biomarkers (BNP, D-dimer, MMP-9, and S100B), but they only found one biomarker, namely BNP, whose levels were considerably higher in IS patients (90.8156.4) as compared to HS patients (16.310.8) and that characterized the two types of stroke with an AUC of 0.61 [58].

1.6 Markers of Brain Injury

Within 2 to 6 hours of the beginning of symptoms, seven studies found that intracerebral hemorrhage (ICH) patients' GFAP levels are considerably higher than those of IS patients [59–64, 66]. Only APC-PCI and GFAP and APC-PCI significantly separated ICH from IS, according to Uden *et al.* 2009's analysis of a panel of biomarkers, including S100B, Neuron Specific Enolase (NSE), GFAP, and Activated Protein C-protein C Inhibitor Complex (APC-PCI), in 83 IS and 14 HS samples. A cutoff value of 0.35 g/l distinguished ICH from IS with a sensitivity of 96% and a specificity of 42%. The APC-PCI levels were much higher in IS patients (0.04–3.55 g/l) than in ICH patients (0.19–0.49 g/l). In ICH patients, GFAP levels were found to be much higher (40–160 ng/l) than in IS patients (30–70 ng/l), and at a cutoff value of 40 ng/l, it was able to distinguish ICH from IS [64, 65]. In a recent study with 146 IS and 46 ICH patients, Luger S *et al.* (2017) found that serum GFAP had a sensitivity of 77.8% and a specificity of 94.2% for separating ICH from IS in less than six hours at a cutoff value of 0.03 g/l [66].

1.7 Therapeutic Advances in Ischemic Stroke

Since well-developed nanomedicines have numerous remarkable benefits, many nanomedicines are developed to increase the effectiveness and decrease the negative effects of conventional cure approaches. Nanomedicine may boost the solubility of ineffectively soluble pharmaceuticals, enhance their steadiness, and lengthen their *in vivo* half-lives [67]. Targeted altered nanomedicine could help medications get around the blood–brain barrier (BBB), which prevents the majority medications from getting to the brain, and achieve collection at the intended spot to prevent unspecified dissemination. Targeted alteration may also make it easier for a given cell type, like damaged neurons, to absorb a nanomedicine. Thus, targeting-capable nanomedicines not only improve curing impact but lowers inserted dose and drug toxicity [68]. The drug delivery systems (DDS), which include stimuli-responsive nanocarriers and targeted nanocarriers, could deliver drugs to desired sites like thrombus and the central nervous system (CNS) and specifically release drugs in those areas by reacting to stimuli that are internal or external, thereby enhancing their therapeutic effects [138]. Additionally, the release of pharmaceuticals might be controlled by nanomedicines made of various functional materials, and the functionalized carrier may be useful in the treatment of ischemic stroke [67].

1.7.1 Ligand-Mediated Active Targeting

Since fibrin is a significant part of thrombus, alteplase was delivered using polystyrene nanoparticles were changed by an antifibrin antibody by combining proteins on their surface. In the absence of an embolus, alteplase NPs displayed significantly lower activity than free enzyme, It would reduce the cleavage of plasminogen in an unspecific manner and raise the likelihood of bleeding less [69]. In addition to single-targeted ligand modification, there are some studies into dual ligand-modified nanomedicine that has superior targeting effectiveness. The contact between thrombocytes is mediated by the overexpressed P-selectin

on active platelets. Dual-targeted nanovesicles modified with cRGD and P-selectin targeting peptide were created to distribute SK105 using this technique as inspiration [70]. Glycerophospholipid-based nanovesicles that were located near the target region were able to release medications in response to stimuli because thrombus-forming platelets and leukocytes overproduce the enzyme phospholipase A₂. may cleave glycerophospholipids [70].

1.7.2 Nanomedicines That Provide Oxygen to Ischemic Brain Tissue

Although hemoglobin (Hb) is a naturally occurring O₂ carrier, its limited clinical use is due to its short half-life and hypertension response [71, 72]. In addition to extending the period that hemoglobin circulates *in vivo*, liposomal hemoglobin (LHb) can transport enough oxygen to go beyond microcirculation's barriers and to the penumbra, where red blood cells (RBCs) are rarely able to reach [73, 74]. When given right away after the middle cerebral artery is blocked, LHb can also greatly reduce the size of the infarction in a transient ischemia model (MCAO) [75, 76].

1.7.3 Reducing Oxidative Stress With Nanomedicines

Small molecule chemicals, antioxidase, and inorganics are the major types of antioxidants used in preclinical research. Antioxidants' pharmacokinetic performance may be enhanced by nanomedicines, which may also help them pass through the BBB and store in the injured brain [77]. Many small molecule antioxidants, including baicalin [78], luteolin [79], curcumin [80], resveratrol [81], tanshinone [82], and puerarin [83], are derived from plants and contain phenolic and keto components. For instance, hydrophobic curcumin is quickly broken down, ejected, and not effectively absorbed by cells *in vivo*. Because cells ingested NPs through endocytosis rather than passive diffusion, more absorption in neurons was seen in PLGA-NPs containing curcumin than in free drug. Additionally, NPs more effectively reduced oxidative stress in H₂O₂-treated neurons [80, 84, 85]. The ability of NPs to prolong curcumin's half-life *in vivo* improved the likelihood that the medication would enter the injured brain during the BBB's opening window. In a different study, exosomes made from embryonic stem cells that had been loaded with curcumin increased the drug's stability and solubility while also addressing the issue of low absorption [86]. Curcumin-loaded embryonic stem cell exosome therapy can therefore considerably lower the level of ROS in the injured brain, decrease the infarct size, and lessen the breakdown of neurovascular units. several manufactured small molecule antioxidants as edaravone [87] and the nitroxyl radicals 2,2,6,6-tetramethylpiperidine-1-oxyl, there are natural antioxidants obtained from plants (TEMPO). The strategy of BBB modification may assist the edaravone micelles achieve more efficient storage in ischemic brain and rescue more neurons. To increase the duration of edaravone's circulation, PEG-PLA micelles that have been treated with CGS21680 were created [88].

1.7.4 Multiple Abnormalities are Controlled by Nanomedicine

Better results are anticipated when numerous abnormalities are suppressed synergistically. Since some medications, like curcumin, have anti-inflammatory, anti-oxidation, and

anti-apoptosis properties, they may be able to control several disorders at once. Additionally, numerous researches have blended various medicines with various roles into nanomedicine to provide combination therapy [67, 89–92]. To distribute the neuroprotectant ZL006 and alteplase, nanoplatelets were created. The TAT-peptide-linked alteplase was attached on the surface of platelet barriers, and the linker could be cleaved by thrombin. ZL006 was precisely inserted into the polymeric NP core. NPs coated with platelets' membranes kept platelets' ability to target thrombin and free out alteplase in response to thrombin's extremely expressed levels in clots. The blocked TAT peptide was then revealed after the linker was broken, which encouraged NPs to penetrate the BBB and distribute ZL006. In MCAO rats, the union of thrombolytics and a neuroprotectant markedly decreased ischemia-related damage [92]. Prior to reperfusion, hypoxia not only results in the depletion of neuronal energy but it causes the formation of ROS; subsequent to reperfusion, an increase in oxygen causes a significant increase in ROS. Manganous tetroxide nanoparticles demonstrated long-lasting ROS scavenging activity. Ischemic brain was saved by controlling O₂ and ROS levels both before and after thrombolysis [92].

Due to their well-developed preparation technology, polymeric NPs, liposomes, and micelles are among the many nanomedicines that are now being studied with the aim of translating them into clinical use. Although inorganic NPs have good consistency and are simple to industrialise, if they are used on humans, considerable more research into their safety is required. Biomimetic nanomedicines, which are based on cell membrane or living cell exosome/vesicles living, have opened up new possibilities for drug targeting delivery in recent years. With the hope of bringing about new advancements in stroke treatment, their distinctive biocompatibility, safety, and intrinsic targeting qualities make them a research hotspot for nanomedicines [93].

1.8 Nanoparticles

1.8.1 Carbon Nanotubes

Graphite sheets tubes with nanoscale widths make to the class of nanomaterials known as carbon nanotubes [8, 94–99]. Their primary medicinal uses include medication delivery, tissue engineering, biosensors, gene therapy, and hormone production [100–104]. As passive diffusion cannot cross the BBB, conjugation of substances that encourage active transport to the brain is crucial for new uses in nanomedicine. Given the special characteristic of carbon nanotubes, they have attracted a lot of attention as nanocarrier systems over the past two decades [105]. Fluorescently tagged multiwalled carbon nanotubes have been discovered to pierce microvascular cerebral endothelium monolayers without significantly harming cerebral endothelial cells, which is a requirement for therapeutic application [106]. Using carbon nanotubes in nanofiber scaffolds has been demonstrated in a recent study to greatly increase neuronal development and differentiation, suggesting potential applications in the field of peripheral nerve rehabilitation [107] (Figure 1.3). Despite the many advantages of carbon nanotubes, there are drawbacks to their use, such as poor water solubility, limited biodegradability and dispersity, harmful drug-induced oxidative stress, and lung illness [108–110].

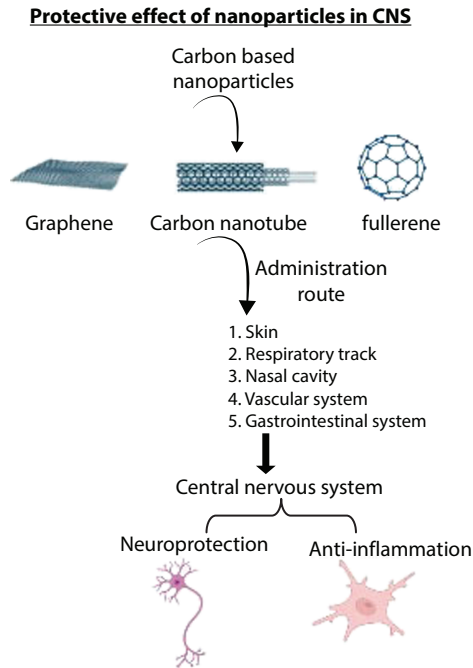


Figure 1.3 It shows the protective effects of carbon-based nanoparticles in central nervous system.

1.8.2 Dendrimers

A class of artificial macromolecules known as dendrimers exhibits a structure like a tree and unique encapsulating characteristics. Interesting structural characteristics of dendrimers include globular and layers of branched nanostructure, as well as a number of terminal functional groups on the outer layer. They may assemble complexes and enclose a variety of molecular entities [111]. Due to their capacity to cross the blood–brain barrier, dendritic macromolecules are commonly utilised in the treatment of illnesses of the central nervous system [112]. Because polyamidoamine, polypropylenimine, and polyacryl ether are utilised in dendrimer formulations and may encapsulate both hydrophilic and hydrophobic compounds, these polymer-based nanostructures are frequently used as nanocarriers to transport different medicinal and imaging agents [113, 114]. The PEGylated dendrimers had the additional benefit of reducing blood clotting, which was helpful in the treatment of stroke. In a mouse model of permanent focal brain ischemia, the brain could also be found to contain the optimised PAMAM formulation 24 hours after injection. PEGylated PAMAM dendrimers extend the half-life of blood circulation and may be used in medication delivery systems [115].

1.8.3 Metal Nanoparticles

Metal nanoparticles are very promising for the therapy and finding disorders of the brain [116–120]. Metal nanoparticles not only have improved photothermal performance but also have superior imaging and detecting capabilities [121–125]. Some metal nanoparticles have magnetic properties, which makes them useful for magnetic hyperthermia, magnetic